Microscopic description of localization-delocalization transitions in $BaFe_2S_3$

L. Craco[1,2] and S. Leoni[3]
[1] *Instituto de Física, Universidade Federal de Mato Grosso, 78060-900, Cuiabá, MT, Brazil*
[2] *IFW Dresden, Institute for Solid State Research, P.O. Box 270116, D-01171 Dresden, Germany*
[3] *School of Chemistry, Cardiff University, Cardiff, CF10 3AT, UK*
(Dated: August 21, 2018)

We present a microscopic description of electronic reconstruction in $BaFe_2S_3$, a system which undergoes a pressure-induced insulator-metal transition followed by a superconducting phase at 24 K. We stress the importance of multi-orbital electron-electron interactions for a consistent understanding of its intrinsic Mott insulating and pressurized, orbital-selective metallic normal states. We explain the first-order nature of the Mott transition, showing that it is driven by dynamical spectral weight transfer in response to changes of on-site Coulomb interaction to bandwidth ratio. As a byproduct of this analysis, we unearth how dynamical correlations underpin spectroscopy and resistivity responses, in good agreement with experiment. Upon electron/hole doping carrier localization is found to persist because the chemical potential lies in a gap structure with vanishing states near the Fermi energy. We detail the implications of our microscopic analysis to the underlying physics which emerges in the normal state of compressed $BaFe_2S_3$ superconductor.

I. INTRODUCTION

The discovery of F-doped LaOFeAs superconductor[1] led to extensive experimental and theoretical study regarding the interplay between electronic structure, magnetism and unconventional high-temperature (high-T_c) superconductivity.[2] Although many families of Fe-based superconductors have been discovered, the majority of these superconducting materials have a two-dimensional Fe-square lattice tetrahedrally coordinated by chalcogen or pnictogen ions. The Fe atoms are nominally divalent (Fe^{2+}) in almost all parent compounds, which usually undergo to magnetic or nematic phase transitions at low temperatures.[3] Superconductivity with $s_{\pm}$ symmetry appears when the striped-type antiferromagnetic ordered state is suppressed by pressure or addition of electron/hole carriers *via* chemical substitution. In spite of the fact that experimentally, various physical responses show distinct features associated with correlated electron physics, there is still significant disagreement concerning the degree of electron correlation effects in the Fe-based superconductors.[2,3] This has resulted in a situation where multi-orbital (MO) electronic structure calculations that explicitly take sizable electron-electron interactions into account were implemented to resolve this crucial issue of fundamental importance.[4] Crucial, because the nature and mechanism of the instability of a metal (strange or not) to a superconductor hinges on whether the normal metal state is conventional Fermi liquid metal or highly unconventional non-Fermi liquid metal in close proximity to Mott localization.

In this context, the discovery of $BaFe_2S_3$, where superconductivity emerges in the vicinity of the Mott insulating state,[5,6] is relevant since it confirms previous theoretical suggestions that Mott-insulating parent compounds in the Fe superconducting systems could be found by tuning the ratio of interaction-to-bandwidth (U/W) below the critical value for a Mott insulator-metal transition.[7] Pressure-induced superconductivity in the Fe-ladder compounds $BaFe_2X_3$ (X =S,Se)[5,6,8] thus focuses the fundamental debate[9] on the degree of electronic correlations in unconventional (non-BCS) superconductors in general. Of particular interest here is $BaFe_2S_3$, a narrow band gap semiconductor[10] with striped-type magnetic ordering below 120 K at ambient pressures, which undergoes a pressure-induced Mott transition followed by superconducting phase at a critical pressure (P_c) of 10.9 GPa.[6]

Before delving into the correlated electronic state that emerges in $BaFe_2S_3$, we recall that the proximity to a Mott metal-insulator transition[11] (Mottness) is a clear manifestation of dynamical many-body effects in correlated electrons. The charge gap at the Mott transition (MT) jumps discontinuously from a finite value to zero. Mott's original idea[12] was to tune the ratio U/W between the on-site Coulomb interaction U and the one-particle bandwidth W (i.e., the kinetic energy of the electrons) which defines the phase boundary between the metallic and the gaped (semiconducting) phase. This scenario holds true for MO systems with similar W values and reduced crystal-field splitting within the active orbitals, but deviations are expected to occur in more general cases where an orbital-selective Mott phase is the precursor to the all-electron Mott insulator.[13] In this work we use local density approximation plus dynamical mean-field theory (LDA+DMFT)[14] to confirm that both localized and itinerant $3d$ electrons coexist[15] in pressurized $BaFe_2S_3$.

The pressure-induced insulator-metal transition in $BaFe_2S_3$ has been characterized as a bandwidth-controlled Mott transition.[5,6] Up to 10.1 GPa the *dc* resistivity shows semiconducting-like behavior and superconductivity at P_c arises directly from a normal state with insulating-like resistivity upturn. Such resistivity upturn, which is followed by a sharp superconducting drop in $BaFe_2S_3$,[6] is a two-particle manifestation of selective localization[16] seen in the Fe-chalcogenide superconductors.[17] Increasing pressure above 11.6 GPa, the resistivity

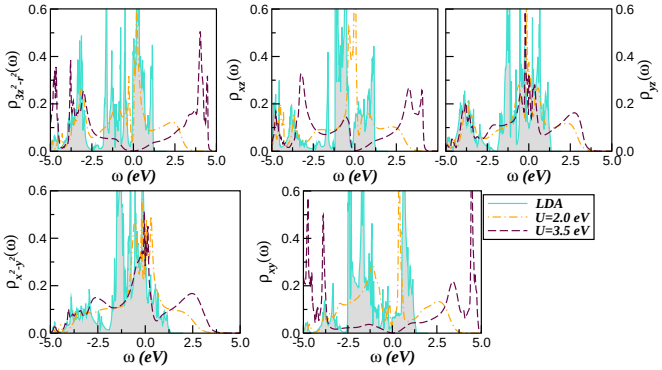

FIG. 1: (Color online) Orbital-resolved LDA and LDA+DMFT density-of-states (DOS) for the Fe 3d-orbitals of paramagnetic $BaFe_2S_3$, showing that all d-bands in LDA span over the Fermi level ($E_F = \omega = 0$). This confirms that the electronic states relevant to orthorhombic Fe-ladder compounds are Fe 3d-states. Noteworthy is the electronic reconstruction with increasing on-site Coulomb interaction and the orbital-selective Mott-Hubbard insulating state with coexisting metallic and insulating bands at E_F for $U = 3.5$ eV.

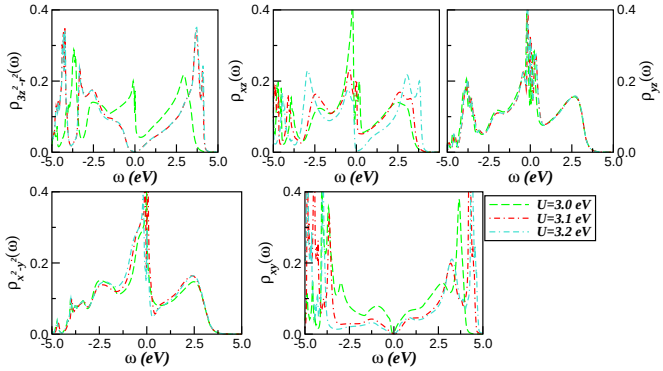

FIG. 2: (Color online) Orbital-resolved LDA+DMFT DOS for the Fe 3d-orbitals across the orbital-selective Mott transition (OSMT) of $BaFe_2S_3$. Large dynamical spectral weight transfer along with abrupt Mott-Hubbard localization is visible in the $3z^2 - r^2, xz, xy$ LDA+DMFT spectral functions.

curves show Fermi-liquid-like T^2 behavior characteristic of a good metal up to about 100 K.[6] However, it turned out that the emergence of superconductivity is sensitive to nominal composition and growth conditions, and that the superconducting signal appears to be maximally enhanced at an slightly off-stoichiometric $BaFe_{2.1}S_3$ compound.[18] Thus, it is plausible to assume that the superconducting state observed in $BaFe_2S_3$ emerges from a combination of bandwidth-control Mott transition[5,6] and doping of electrons into the iron network.[19] With this in mind, in this work we explore the role played by these two cooperative antilocalization effects,[11] showing that the Mott insulating state is rather robust against small changes in electron concentration of the Fe-3d shell.

II. METHOD

Within the orthorhombic (space group $Cmcm$) crystal structure (see Fig. **??**) and using lattice constants and atomic positions at ambient pressure conditions,[18] one-electron band structure LDA calculations were performed for $BaFe_2S_3$ using the linear muffin-tin orbitals (LMTO) scheme in the atomic sphere approximation[21]: Self-consistency is reached by performing calculations with 657 irreducible **k**-points. The radii of the atomic spheres were chosen as r=4.95 (Ba), r=2.57 (Fe) and r=2.7 (S) a.u. in order to minimize their overlap. Consistent with previous density functional calculations for $BaFe_2S_3$ parent compound[20] our LDA results in Fig. 1 confirms that the active electronic states in this 123-spin-ladder compound involve the Fe 3d carriers, where all d-bands have appreciable weight near E_F. From LDA, the one-electron part of the MO Hamiltonian for $BaFe_2S_3$ is $H_0 = \sum_{\mathbf{k},a,\sigma} \epsilon_a(\mathbf{k}) c^\dagger_{\mathbf{k},a,\sigma} c_{\mathbf{k},a,\sigma}$, where $a = (x^2-y^2, 3z^2-r^2, xz, yz, xy)$ denote its diagonalized 3d orbitals and $\epsilon_a(\mathbf{k})$ is the corresponding band dispersion, which encodes details of the one-electron (LDA) band structure. These five Fe-3d bands are the relevant one-particle inputs for MO-DMFT which generates a first order Mott-Hubbard insulating state at $U =$ 4.5 eV as shown below. Similar to tetragonal Fe-based superconductors,[4] the correlated many-body Hamiltonian for $BaFe_2S_3$ reads $H_{int} = U \sum_{i,a} n_{i,a,\uparrow} n_{i,a,\downarrow} + U' \sum_{i,a\neq b} n_{i,a} n_{i,b} - J_H \sum_{i,a\neq b} \mathbf{S}_{i,a} \cdot \mathbf{S}_{i,b}$. Here U is the on-site Coulomb interaction, $U' = U - 2J_H$ is the inter-orbital Coulomb interaction term, and J_H is the Hund's coupling. We evaluate the many-particle Green's functions $[G_{a,\sigma}(\mathbf{k},\omega)]$ of the MO Hamiltonian $H = H_0 + H_{int}$ within LDA+DMFT,[14] using MO iterated perturbation theory (MO-IPT) as impurity solver.[22] The DMFT solution involves replacing the lattice model by a self-consistently embedded MO-Anderson impurity model, and the self-consistency condition requiring the local impurity Green's function to be equal to the local Green's function for the lattice. The full set of equations for the MO case can be found in Ref. 22.

III. RESULTS AND DISCUSSION

In Fig. 1 we display the effect of moderate[15,20] electron-electron interactions on the orbital-resolved spectral functions of $BaFe_2S_3$ parent compound within the d^6 electronic configuration. At U =2.0 eV the system is a Fermi-liquid metal, where all orbital display appreciable spectral weight at E_F. In spite of this small U value, lower (LHB) and upper (UHB) Hubbard bands are visible in all orbitals, suggesting an intrinsic tendency towards localization in this and related ladder compounds. Be-

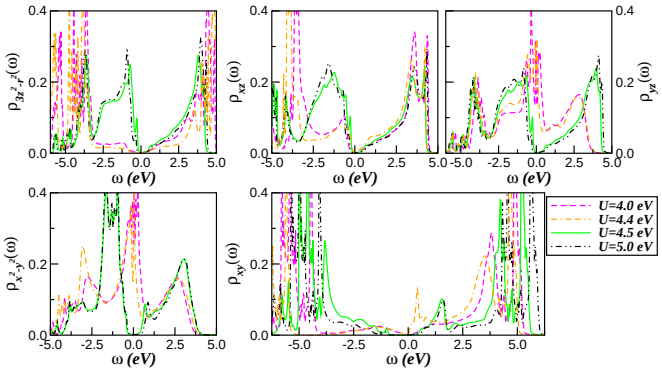

FIG. 3: (Color online) Orbital-resolved LDA+DMFT DOS for the Fe 3d-orbitals of $BaFe_2S_3$ across the second first-order, orbital-selective metal-insulator transition. Large dynamical spectral weight transfer along with Mott-Hubbard localization on all active is visible in the LDA+DMFT spectral functions at the critical phase boundary, $4.4 < U_{MT} < 4.5$ eV.

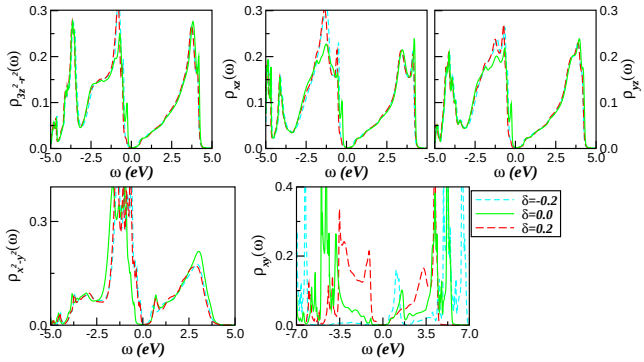

FIG. 4: (Color online) Evolution of the LDA+DMFT ($U = 4.5$ eV, $J_H = 0.7$ eV) orbital-resolved spectral functions of $BaFe_2S_3$ for different values of the total band filling of the Fe 3d-shell, $n_t = 6 \pm \delta$. Notice the modification of the xy density-of-states due to large-scale dynamical spectral weight transfer with δ. While all orbitals remain Mott localized, incoherent valence-band states with $x^2 - y^2$ orbital character almost touch E_F due to doping-induced selective-orbital reconstruction in $BaFe_2S_3$.

tween $3.1 < U < 3.2$ eV (and $J_H = 0.7$ eV) a first-order phase transition from a metallic to an orbital-selective Mott state[13] takes place, where the $3z^2 - r^2, xz, xy$ orbitals are Mott localized whereas $yz, x^2 - y^2$ remain metallic. Strong electronic reconstruction sets in within the selective-Mott-localized orbitals, with the concomitant formation of localized moments (LHB) at energies below -2.5 eV. Both the energy position of the Hubbard bands and the size of the Mott gap are found to be orbital dependent, and this anisotropic electronic state could be probed in future transport and spectroscopy experiments of pressurized $BaFe_2S_3$ with partially quenched electron correlation effects. Taken together, our results in Fig. 1 confirm that itinerant and Mott-localized electrons coexist in the orbital-selective Mott state[23] of $BaFe_2S_3$.

For a more detailed analysis of dynamical MO electronic interaction effects near the orbital-selective phase transition of $BaFe_2S_3$ at moderate U values, we show the orbital-resolved spectral functions in Fig. 2. Electronic correlations lead to interesting modifications of the correlated spectra. Below the critical value for the orbital-selective insulating phase ($3.1 < U_{OS} < 3.2$ eV) the many-body spectra describe the coexistence of metallic $(yz, x^2 - y^2)$ and Mott localized $(3z^2 - r^2, xz, xy)$ electronic states. Noteworthy is the abrupt electron localization within the $3z^2 - r^2, xz$ orbitals and its coexistence with a quasi-coherent $x^2 - y^2, yz$ electronic fluid. Albeit near U_{OS} eV only gradual changes are seen in the spectral function of the $x^2 - y^2, yz$ orbitals, the LDA+DMFT DOS of the $3z^2 - r^2, xz$ and xy orbitals show large changes in spectral weight transfer (SWT) at the orbital-selective critical phase boundary in $BaFe_2S_3$: The concomitant formation of incipient $(x^2 - y^2, yz)$ and narrow $(3z^2 - r^2, xz)$ Hubbard bands at energies above 2.0 eV in Fig. 2 are one-particle fingerprints of selective Mottness intrinsic to correlated multi-orbital systems.

Similar to other Fe-chalcogenide systems,[13,24] a first order transition from an orbital-selective metallic state to a correlated Mott insulator (MI) with increasing U is obtained for $BaFe_2S_3$ (Fig. 3). At $U_{MT} = 4.5$ eV (and $J_H = 0.7$ eV) $BaFe_2S_3$ is a MO Mott-Hubbard insulator with an orbital dependent band gap. Hubbard bands are visible, albeit to a different extent in all orbital-resolved spectral functions. As seen in Fig. 3, in this orbital-blocked Mott state the $xy, x^2 - y^2$ orbitals show stronger correlation effects with pronounced Hubbard bands while the $3z^2 - r^2, xz, yz$ orbitals have less tendency towards local moment formation. Noteworthy as well is the appearance of the one-electron dispersion at low binding energies within the $3z^2 - r^2, xz, yz$ orbitals at U_{MT}, a fingerprint of distinct electronic anisotropies within the Fe 3d shell.[25] Large-scale changes in SWT thus characterizes the Mott transition in $BaFe_2S_3$. The orbital-resolved LDA+DMFT spectral functions are predicted to be highly reshaped by electron-electron interactions and future PES and XAS experiments could verify this aspect.

What happens with the orbital-blocked phase in Fig. 3 upon doping? Even though data exists,[18] the robustness of the Mott insulating state and the instabilities of such state to unconventional order, and, in particular, to high-T_c superconductivity makes this an important question to inquire about. In Fig. 4 we show the changes in the correlated electronic structure upon doping ($n_t \equiv 6 \pm 0.2$) the Mott insulator. Consistent with extant transport data,[18] the localization-delocalization transition does not occur at small doping. What is the origin of this persistent localized behavior in doped $BaFe_2S_3$? In Mott localized Fe-chalcogenide systems[27] strong incoherent scattering between different carriers in orbital states split relative to each other due to the specific crystal-field leads

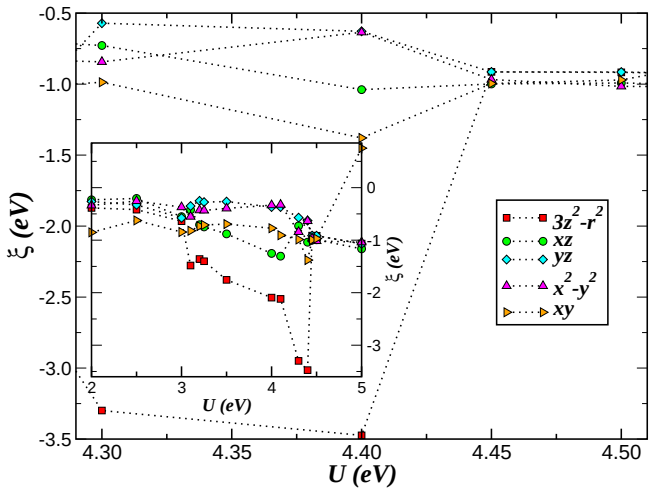

FIG. 5: (Color online) U-dependence of the gravity centers for the different LDA+DMFT bands, showing that $3z^2-r^2$ is the ground state orbital of metallic $BaFe_2S_3$ at the border of the pressure-induced Mott transition. Particular interesting features are the changes in the renormalized orbital splittings due to large spectral weight transfer and the two-fold (yz, x^2-y^2) orbital degeneracy at U=4.4 eV. The latter suggests a two-orbital pairing mechanism near P_c similar to tetragonal Fe-superconductors.[26]

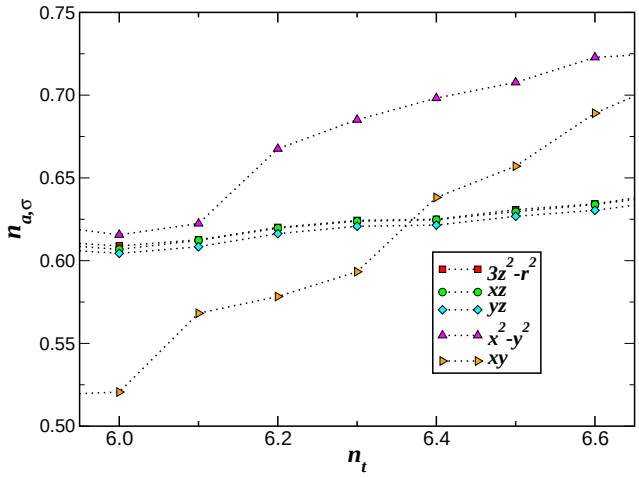

FIG. 6: (Color online) Evolution of the Fe-3d orbital occupations ($n_{a,\sigma}$) with increasing the total Fe-band filling ($n_t = 6+\delta$) for $U = 4.5$ eV and $J_H = 0.7$ eV, showing enhanced charge carrier concentration and orbital polarization within the x^2-y^2, xy orbitals upon electron doping the parent compound.

to two main effects: It leads, via static-Hartree contributions (from the static part of the orbital-dependent self-energies) to an-orbital-dependent shifts of the 3d-bands relative to each other (see Fig. 5) and strong dynamical correlations due to sizable U and U' cause appreciable spectral weight transfer over large energy scales, from high to low-energy, upon carrier doping. This second feature leads to a drastic modification of the spectral lineshape of the xy orbital as shown in Fig. 4.

Finally, motivated by the fact that the superconducting state observed in $BaFe_2S_3$ seems to emerge from a combination of bandwidth-control Mott transition[5,6] and doping of electrons into the iron network,[18,19] in Fig. 6 we display the averaged occupation number of each orbital, $n_{a,\sigma} \equiv < n_{a,\sigma} >$, computed using the LDA+DMFT orbital-resolved spectral functions of $BaFe_2S_3$ for $U = 4.5$ eV and $J_H = 0.7$ eV. Our results suggest strong orbital differentiation[28] between out-of-plane $(3x^2-r^2, xz, yz)$ and in-plane (x^2-y^2, xy) orbitals and enhanced charge carrier concentration within the ladder in-plane orbitals with increasing δ. This response is characteristic of strongly correlated materials, where the orbital differentiation is linked to charge and orbital excitations[29] in the reconstructed electronic state at low temperatures. Noteworthy here is the fact that in this selective regime some of the active orbitals might get decoupled from the others,[13] as seen in our results for the xy orbital in Figs. 2 and 3. Interestingly, this marked behavior is consistent with that found in model calculations for alkaline Fe selenides,[13] where the xy orbital is the most localized since it is found to be very close to half-filling as shown in Fig. 6 for $n_t \approx 6.0$. As a byproduct of this analysis and similar to our earlier LDA+DMFT study on insulator-metal transition in high-pressure oxygen,[30] we propose that changes in $n_{a,\sigma}$ would induce anisotropic small variations in lattice parameters upon doping the parent compound. Though not probed yet, we predict that the lattice parameters along the ladder plane will increase, while the perpendicular one is expected to remain almost constant as in Fig. 6.

For a more detailed analysis of dynamical MO electronic interaction effects in $BaFe_2S_3$, in Fig. 7 we compare our LDA+DMFT result with extant UPS spectroscopy data.[15] Since only the five 3d-bands have been included in the LDA+DMFT treatment, we restrict ourselves to the energy window up to 1.5 eV binding energy, where only the five 3d-bands dominate in LDA. Good quantitative agreement with UPS result is obtained at low energies. In particular, the bump feature at -0.85 eV and the low-energy lineshape are faithfully reproduced for electron doped (δ=0.2) $BaFe_2Se_3$. Taken together with our earlier results,[27,31] this confirms that iron 3d states with sizable to strong MO correlations are a universal feature among Mott localized Fe-chalcogenides. Hence, our results for the total spectral function shown in the inset of Fig. 7 constitute a quantitative rationalization of basic one-particle responses of doped 123-spin-ladder Fe-chalcogenides and serve as a basis to explore the electronic reconstruction upon doping[18,19] the parent compound.

In earlier works we have shown that the MO correlated nature of different Fe-chalcogenide systems[24,27,31] can be semiquantitatively understood using LDA+DMFT with

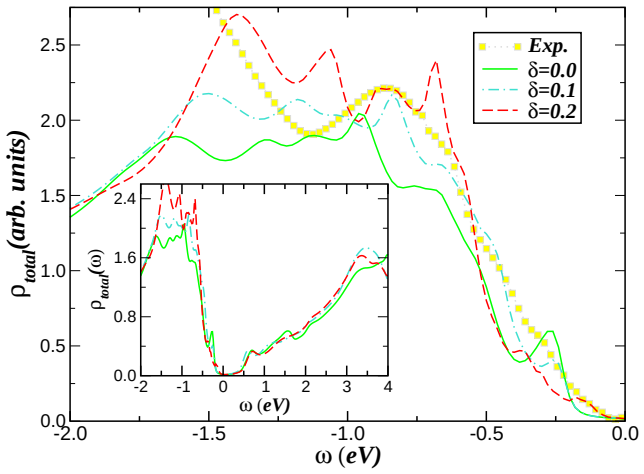

FIG. 7: (Color online) Comparison between the LDA+DMFT result for pure and doped $BaFe_2S_3$ and ultraviolet photoemission spectra (UPS, squares) taken from Ref. 15. Good quantitative theory-experiment agreement up 1.5 eV binding energy is visible. In particular, the low-energy lineshape and the bump feature around -0.85 eV are accurately resolved in the LDA+DMFT spectrum for electron doped ($\delta = 0.2$) $BaFe_3S_3$. Inset shows the doping dependence of LDA+DMFT conduction band states which might be probed in future inverse photoemission spectroscopy experiments.

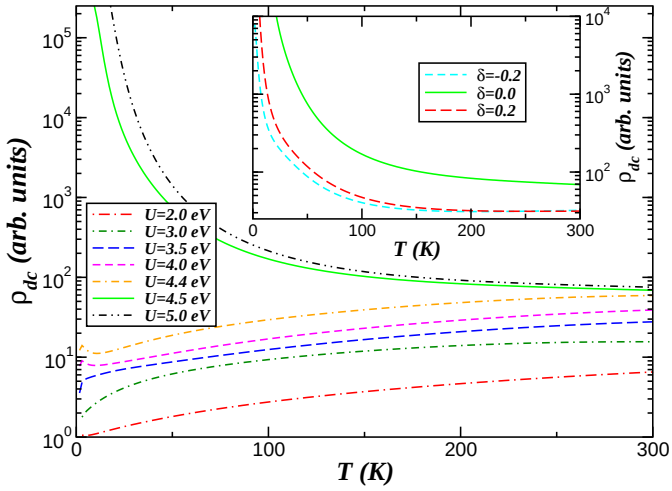

FIG. 8: (Color online) T-dependence of electrical resistivities for Mott-insulating and metallic $BaFe_2S_3$, showing qualitative good accord with transport data.[5,6] Particularly interesting is the first order metallic-to-semiconducting behavior for 4.4 eV$\leq U \leq$ 4.5 eV consistent with normal state data of Ref. 6. Inset display resistivity curves for $U_{MT} = 4.5$ eV and different total band filling, showing that the Mott insulating state is rather robust against small electron/hole doping.

sizable to strong d-band correlations. Here, we extend this aspect to characterize the electrical properties of $BaFe_2S_3$ and its link to orbital-selective Mottness under pressure. Specifically, we study the T-dependence of the dc resistivity and correlate it with the orbital-reconstruction scenario derived above. Given the correlated spectral functions $A_a(\mathbf{k},\omega) = -\frac{1}{\pi} ImG_a(\mathbf{k},\omega)$ the (static) dc conductivity $[\sigma_{dc}(T)]$, computed within the DMFT formalism[32], can be expressed as $\sigma_{dc}(T) = \frac{\pi}{T}\sum_a \int d\epsilon \rho_a^{(0)}(\epsilon) \int d\omega A_a^2(\epsilon,\omega) f(\omega)[1-f(\omega)]$. In this expression, $\rho_a^{(0)}(\epsilon)$ is the LDA DOS of the a-bands (Fig. 1) and $f(\omega)$ is the Fermi function.

In Fig. 8 we display the T-dependence of electrical resistivity $[\rho_{dc}(T) \equiv 1/\sigma_{dc}(T])$ with increasing U, computed using the LDA+DMFT orbital resolved spectral functions for in $\sigma_{dc}(T)$. Various interesting features immediately stand out. First, $\rho_{dc}(T \to 0)$ is large with clear insulating like behavior at $U \geq 4.5$ eV, in accordance with the Mott insulating description above. This Mott-localized behavior is first order suppressed in the orbital-selective metallic phase at $U = 4.4$ eV. From this critical value to 4.0 eV the resistivity curves show a small insulating upturn below 10 K. While this resistivity upturn appears around 80 K in pressurized $BaFe_3S_3$,[5,6] the detailed T-dependence in Fig. 8 resembles the one seen in experiment, showing first order insulator-metal transition[6] with increasing pressure from ambient to 10.9 GPa. With further reducing the effective U/W ratio, or by increasing the one-particle bandwidth W with pressure,[11] a crossover from a bad-metallic to a Fermi liquid behavior (at U=2.0 eV) is observed in $\rho_{dc}(T)$. Finally in the inset of Fig. 8 we display the effect of doping the parent compound, showing reduced resistivity, albeit still insulating, consistent with experimental observations in electron and hole doped $BaFe_3S_3$. A particularly interesting feature to be seen is the reduced resistivity for hole-doping compared to electron-doping which nicely agrees with experimental observations.[18]

To rationalize the overall bad-insulating behavior, which is characterized by a small resistivity upturn at low temperatures at the border of the bandwidth-controlled Mott transition[5,6] in pressurized $BaFe_2S_3$, the selective-localization of $3x^2 - r^2, xz, xy$ electronic states below U_c in Fig. 3 implies that these orbital act like an intrinsic source of electronic disorder in the system. This implies that an intrinsic disorder potential, arising from orbital-selective Mott physics, exists in $BaFe_2S_3$ at pressures close to P_c. Remarkably, such behavior results from strong scattering between effectively Mott-localized and itinerant components of the full DMFT propagators. This is intimately linked to orbital-selective Mott-like physics within DMFT.[33] We note that such orbital-selective physics has also been proposed earlier for hexagonal iron-chalcogenides[34] as well as on phenomenological grounds for iron-pnictides superconductors.[35] The qualitative agreement between our resistivity results close to P_c and that seen in experiments,[6] suggests appreciable orbital reconstruction at low-binding energies and persistent Mott localization within the xy orbital sector and future theoretical and experimental work to corroborate

our prediction are called for. Here, we emphasize that coexistence of insulating $(3z^2 - r^2, xz, xy)$ and metallic $(yz, x^2 - y^2)$ states at $3.2 < U_{OS} < 4.4$ eV is the key mechanistic step, which allows to understand the strange metallic behavior observed at pressure range between 11.6 to 13.4 GPa in $BaFe_2S_3$.[5,6] Hence, it would be interesting to see whether this selective orbital mechanism with quasiparticle resonances coexisting with Mott localized electronic states near E_F would be observable in angle-resolved PES (ARPES) spectroscopy of pressurized $BaFe_2S_3$.

IV. CONCLUSION

In summary, we have used LDA+DMFT on a five-band Hubbard model to derive a correlation-induced orbital reconstruction in the spin-ladder compound $BaFe_3S_3$. We have analyzed its Mott-insulating nature, baring it as an effect of multi-orbital dynamical correlations. Upon consideration of reduced correlations effects (due to broadening of the electronic bandwidth by pressure)[20] we observe two distinct first order phase transitions. The first, which is relevant to experiments at moderate pressure conditions, is shown to be of selective Mott type where localized and itinerant electrons coexist in the non-magnetically ordered normal state. Approaching the weak coupling regime we predict an abrupt transition from an orbital-selective Mott phase to a Fermi liquid metal, which is accompanied by large changes in dynamical spectral weight transfer at high- and low-energies.

Acknowledgments

L.C.'s work is supported by CNPq (Grant No. 304035/2017-3). S.L. acknowledges support from the UK Research Council for using work in the paper that was undertaken by a student under Project No. EP/M50631X/1 as well as the DFG for support under the priority project SPP1415 and for a personal Heisenberg grant. S.L. also thanks ARCCA Cardiff for computational resources. Via S.L.'s membership of the UK's HPC Materials Chemistry Consortium, which is funded by EPSRC (No. EP/L000202), this work made use of the facilities of ARCHER, the UK's National High-Performance Computing Service, which is funded by the Office of Science and Technology through EPSRC's High End Computing Programme.

[1] Y. Kamihara, T. Watanabe, M. Hirano, and H. Hosono, J. Am. Chem. Soc. 130, 3296 (2008).
[2] D. C. Johnston, Advances in Physics **59**, 803 (2010); G. R. Stewart, Rev. Mod. Phys. **83**, 158 (2011); Q. Si, R. Yu, and E. Abrahams, Nat. Rev. Mater. **1**, 16017 (2016).
[3] M. Yi, Y. Zhang, Z.-X. Shen, and D. Lu, Quantum Materials **2**, 57 (2017).
[4] K. Haule, J. H. Shim, and G. Kotliar, Phys. Rev. Lett. **100**, 226402 (2008); L. Craco, M. S. Laad, S. Leoni, and H. Rosner, Phys. Rev. B **78**, 134511 (2008).
[5] H. Takahashi, A. Sugimoto, Y. Nambu, T. Yamauchi, Y.Hirata, T. Kawakami, M. Avdeev, K. Matsubayashi, F. Du, C. Kawashima, H. Soeda, S. Nakano, Y. Uwatoko, Y. Ueda, T. J. Sato, and K. Ohgushi, Nat. Mater. **14**, 1008 (2015).
[6] T. Yamauchi, Y. Hirata, Y. Ueda, and K. Ohgushi Phys. Rev. Lett. **115**, 246402 (2015).
[7] G. Baskaran, J. Phys. Soc. Jpn. **77**, 113713 (2008); R. Yu, J.-X. Zhu, and Q. Si, Phys. Rev. Lett. **106**, 186401 (2011).
[8] J. Ying, H. Lei, C. Petrovic, Y. Xiao, and V. V. Struzhkin, Phys. Rev. B **95**, 241109(R) (2017).
[9] Q. Si, Nature Phys. **5**, 629 (2009); M. M. Qazilbash, J. J. Hamlin, R. E. Baumbach, L. Zhang, D. J. Singh, M. B. Maple, D. N. Basov, Nature Phys. **5**, 647 (2009).
[10] W. M. Reiff, I. E. Grey, A. Fan, Z. Eliezer, and H. Steinfink, J. Solid State Chem. **13**, 32 (1975); Z. S. Gönen, P. Fournier, V. Smolyaninova, R. Greene, F. M. Araujo-Moreira, and B. Eichhorn, Chem. Mater. **12**, 3331 (2000).
[11] M. Imada, A. Fujimori, and Y. Tokura, Rev. Mod. Phys. **70**, 1039 (1998).
[12] N. F. Mott, Metal-Insulator Transitions (Taylor and Francis, London, 1974).
[13] R. Yu and Q. Si, Phys. Rev. Lett. **110**, 146402 (2013).
[14] G. Kotliar, S. Y. Savrasov, K. Haule, V. S. Oudovenko, O. Parcollet, and C. A. Marianetti, Rev. Mod. Phys. **78**, 865 (2006).
[15] D. Ootsuki, N. L. Saini, F. Du, Y. Hirata, K. Ohgushi, Y. Ueda, and T. Mizokawa, Phys. Rev. B **91**, 014505 (2015).
[16] L. Craco, M. S. Laad, and S. Leoni, Europhys. Letters **91**, 27001 (2010); L. Craco, Solid State Comm. **253**, 14 (2017).
[17] T. J. Liu, X. Ke, B. Qian, J. Hu, D. Fobes, E. K. Vehstedt, H. Pham, J. H. Yang, M. H. Fang, L. Spinu, P. Schiffer, Y. Liu, and Z. Q. Mao, Phys. Rev. B **80**, 174509 (2009); Y. Mizuguchi, F. Tomioka, S. Tsuda, T. Yamaguchi, and Y. Takano, J. Phys. Soc. Jpn. **78**, 074712 (2009); M. H. Fang, J. H. Yang, F. F. Balakirev, Y. Kohama, J. Singleton, B. Qian, Z. Q. Mao, H.D. Wang, and H.Q. Yuan, Phys. Rev. B **81**, 020509 (2010).
[18] Y. Hirata, S. Maki, J.-I. Yamaura, T. Yamauchi, and K. Ohgushi, Phys. Rev. B **92**, 205109 (2015).
[19] Y. Zhang, L. Lin, J.-J. Zhang, E. Dagotto, and S. Dong, Phys. Rev. B **95**, 115154 (2017).
[20] R. Arita, H. Ikeda, S. Sakai, and M.-T. Suzuki, Phys. Rev. B **92**, 054515 (2015).
[21] O. K. Andersen, Phys. Rev. B **12**, 3060 (1975). For the implementation of the LMTO scheme see V. Antonov, B. Harmon, and A. Yaresko, *Electronic structure and magneto-optical properties of solids* (Kluwer Academic Publishers (Dordrecht, Boston, London), 2004).
[22] L. Craco, Phys. Rev. B **77**, 125122 (2008).
[23] M. Mourigal, S. Wu, M.B. Stone, J.R. Neilson, J.M. Caron, T.M. McQueen, and C.L. Broholm, Phys. Rev. Lett. **115**, 047401 (2015).
[24] B. Freelon, Y. Hao Liu, J.-L. Chen, L. Craco, M. S. Laad,

S. Leoni, J. Chen, L. Tao, H. Wang, R. Flauca, Z. Yamani, M. Fang, C. Chang, J.-H. Guo, and Z. Hussain, Phys. Rev. B **92**, 155139 (2015); L. Craco and S. Leoni, Scientific Reports **7**, 46439 (2017).

[25] K. Takubo, Y. Yokoyama, H. Wadati, S. Iwasaki, T. Mizokawa, T. Boyko, R. Sutarto, F. He, K. Hashizume, S. Imaizumi, T. Aoyama, Y. Imai, and K. Ohgushi, Phys. Rev. B **96**, 115157 (2017).

[26] M. S. Laad and L. Craco, Phys. Rev. Lett. **103**, 017002 (2009).

[27] L. Craco, M. S. Laad, and S. Leoni, J. Phys.: Condens. Matter. **26**, 145602 (2014).

[28] See, Z. Wang, M. Schmidt, J. Fisher, V. Tsurkan, M. Greger, D. Vollhardt, A. Loidl, and J. Deisenhofer, Nature Communications **5**, 3202 (2014) and references therein.

[29] N. D. Patel, A. Nocera, G. Alvarez, A. Moreo, S. Johnston, and E. Dagotto, arXiv:1807.10419.

[30] L. Craco, M. S. Laad, and S. Leoni, Sci. Rep., **7**, 2632 (2017).

[31] L. Craco, M. S. Laad, and S. Leoni, Phys. Rev. B **84**, 224520 (2011).

[32] K. Haule and G. Kotliar, New. J. Phys. **11**, 025021 (2009).

[33] S. Biermann, L. de Medici, and A. Georges, Phys. Rev. Lett. **95**, 206401 (2005); M. S. Laad, L. Craco, and E. Müller-Hartmann, Phys. Rev. B **73**, 045109 (2006).

[34] L. Craco and S. Leoni, Europhys. Lett. **92**, 67003 (2010); L. Craco, J. L. B. Faria, and S. Leoni, Mater. Res. Express **4**, 036303 (2017).

[35] A. Hackl and M. Vojta, New J. Phys. **11**, 055064 (2009).